Journal of Atmospheric and Solar-Terrestrial Physics 70 (2008) 1894–1903

Contents lists available at ScienceDirect

Journal of Atmospheric and Solar-Terrestrial Physics

journal homepage: www.elsevier.com/locate/jastp

Large-scale ionospheric gradients over Europe observed in October 2003

N. Jakowski [a,*], J. Mielich [b], C. Borries [a], L. Cander [c], A. Krankowski [d], B. Nava [e], S.M. Stankov [a]

[a] Institute of Communications and Navigation, German Aerospace Center, Kalkhorstweg 53, D-17235 Neustrelitz, Germany
[b] Institute of Atmospheric Physics, University of Rostock, Juliusruh, Germany
[c] Radio Communications Research Unit, Rutherford Appleton Laboratory, Chilton, Didcot, Oxon OX11 0QX, UK
[d] Institute of Geodesy, University of Warmia and Mazury, Olsztyn, Poland
[e] Aeronomy and Radiopropagation Laboratory, Abdus Salam ICTP, 34100 Trieste, Italy

ARTICLE INFO

Article history:
Accepted 23 March 2008
Available online 20 April 2008

Keywords:
Ionosphere
Perturbations
Ionosonde
GPS

ABSTRACT

It is well known that ionospheric perturbations are characterised by strong horizontal gradients and rapid changes of the ionisation. Thus, space weather induced severe ionosphere perturbations can cause serious technological problems in Global Navigation Satellite Systems (GNSS) such as GPS. During the severe ionosphere storm period of 29–31 October 2003, reported were several significant malfunctions due to the adverse effects of the ionosphere perturbations such as interruption of the WAAS service and degradation of mid-latitudes GPS reference services. To properly warn service users of such effects, a quick evaluation of the current signal propagation conditions expressed in a suitable ionospheric perturbation index would be of great benefit. Preliminary results of a comparative study of ionospheric gradients including vertical sounding and Total Electron Content (TEC) data are presented. Strong enhancements of latitudinal gradients and temporal changes of the ionisation are observed over Europe during the 29–30 October storm period. The potential use of spatial gradients and rate of change of foF2 and TEC characterising the actual perturbation degree of the ionosphere is discussed. It has been found that perturbation induced spatial gradients of TEC and foF2 strongly enhance during the ionospheric storm on 29 October over the Central European region in particular in North–South direction exceeding the gradients in East–West direction by a factor of 2.

1. Introduction

Severe ionospheric perturbations and related spatial gradients and rapid changes of electron density can seriously degrade the performance of GPS reference network services (e.g. Skone et al., 2001; Jakowski et al., 2005; Stankov et al., 2006). To warn users of commercial services in a proper way, the availability of a simple index number characterising the current signal propagation conditions would be of great benefit (Jakowski et al., 2006). Space Weather monitoring, modelling and forecast refer to a great extent to activity indices such as the Zurich sunspot number Rz and the 10.7 cm radio flux index F10.7 both characterising the solar activity and the geomagnetic indices K_p, A_p, D_{st} providing a measure of the geomagnetic activity (Menvielle and Berthelier, 1991). There is a serious practical reason for using such indices because the index provides a quick and proxy measure of a complex and essential behaviour of the considered subject.

Although it has been shown in many publications that ionospheric perturbations are closely correlated with geomagnetic indices, ionospheric perturbations cannot

* Corresponding author.
E-mail address: norbert.jakowski@dlr.de (N. Jakowski).

1364-6826/$ - see front matter © 2008 Elsevier Ltd. All rights reserved.
doi:10.1016/j.jastp.2008.03.020

be sufficiently described by geomagnetic activity indices. This is due to their complex nonlinear interaction with the thermospheric and magnetospheric processes (e.g. Cander, 1993; Cander and Mihajlovic, 1998). Thus, to describe essential features of ionospheric perturbations in operational applications, it is suggested that specific ionospheric perturbation indices are to be developed (Jakowski et al., 2005; Bremer et al., 2006). Considering the technical needs of real-time Global Navigation Satellite Systems (GNSS) applications, favourite candidates for such indices should measure the local or integrated electron density and its spatial gradients and temporal changes. Although indices give a simplified description of plasma production, loss and transport processes and their coupling e.g. with thermospheric and magnetospheric processes they must have a clear physical meaning and a clear definition. This guarantees that the index is an objective and unambiguous measure.

The aim of this paper is to study the behaviour of some selected ionospheric parameters describing spatial plasma density gradients and their variability over a full month. The potential for using these quantities as perturbation indices is discussed. Well-defined indices could be valuable for an early disturbance warning and monitoring that serves both the scientific research and operational communities. To enable a comparison between quiet and strong perturbed conditions, we analyse vertical sounding and TEC data over Europe during the month of October 2003. The European COST 296 action (Mitigation of Ionospheric Effects on Radio Systems—MIERS, http://www.cost296.rl.ac.uk/) provides an opportunity for organising international measuring campaigns and coordinated data analyses. To investigate possibilities of describing ionospheric perturbations by such an index, a task force group was established earlier in the COST 296 activity.

2. Data base

2.1. Vertical sounding data

Current information technologies have brought a significant change in the ionosonde networks that now in most cases routinely deliver real- or near real-time ionospheric data to be used in the communication and navigation decision-making systems of high complexity. As space weather prediction systems started to rely considerably on this geophysical information, it is necessary to study their applicability in a process of defining an ionospheric perturbation index. The measurements in this paper were obtained by ionosondes sited at European mid-latitude stations during October 2003 (see Fig. 1 and Table 1). The foF2 database contains all automatically scaled vertical incidence ionograms taken from various data centres listed up in the references. Only Sodankyla foF2 data are manually scaled.

The basic operational time resolution of ionosonde data is $\Delta t_{VS} = 15$ min. Since not all ionosonde stations provide 15 min data for October 2003, the gaps of missing data were filled in by interpolated values (see Table 1). At this stage of the perturbation index development, the consideration has not been given to the quality control of automatically scaled vertical incidence ionosonde data (Conkright and McNamara, 1997).

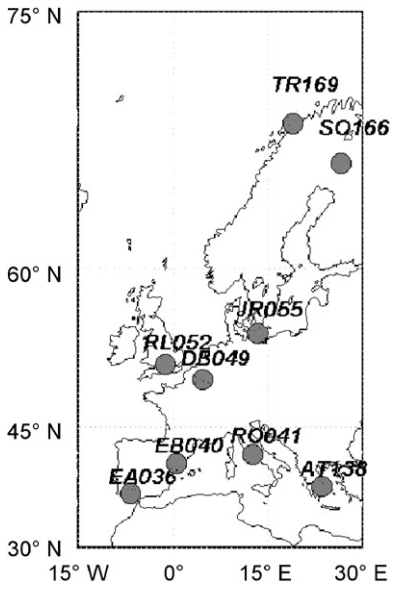

Fig. 1. Ionosonde station sites used for computing horizontal ionisation gradients (circles).

2.2. Total Electron Content data

To derive the Total Electron Content (TEC) of the ionosphere from ground-based GPS measurements, various techniques have been developed. In this study, TEC data are provided from DLR/Neustrelitz (e.g. Jakowski, 1996) and University of Warmia and Mazury (UWM) in Olsztyn (Baran et al., 1997). Basically, the computation of TEC includes the following procedures:

- Computation of the differential delays of code and carrier phases along all available GPS-receiver radio links.
- Calibration of the biased TEC values, which are proportional to the differential delays. Strictly speaking, there is one bias for each satellite and for each station. Usually, the calibration requires a simplified ionospheric model e.g. by a polynomial approach.
- Mapping the calibrated TEC to the vertical at the pierce point of the ray path with a single-layer mapping function at a fixed height between 300 and 450 km.
- Construction of TEC maps from individual TEC measurements distributed over a certain region or on global scale.

TEC is regularly processed in DLR from GPS ground stations of the International GNSS Service IGS since 1995, thus covering more than one solar cycle. The 30 s data of GPS stations allow the determination of slant TEC values along numerous satellite-receiver links over the European area ($32.5^\circ < \varphi < 70^\circ$N; $-20^\circ < \lambda < 40^\circ$E). Both the TEC and

Table 1
Geographical coordinates and URSI station codes of the ionosonde stations used in this study with corresponding data availability and methods used to obtain missing data for a required time resolution of 15 min in October 2003

Station name	URSI station code	Geographical coordinates	Time resolution of sounding measurements (min)	Method of missing data usage[a]
Chilton	RL052	51.60°N; 358.70°E	10	15 min, linearly interpolated between 10/20 and 40/50 min
Juliusruh	JR055	54.60°N; 13.40°E	15	
Rome	RO041	41.90°N; 12.52°E	15	
Athens	AT138	38.00°N; 23.60°E	5/15	Night—5 min, day—15 min
Tromso	TR169	69.70°N; 19.00°E	60	15 min linear interpolated
El_Arenosillo	EA036	37.10°N; 353.27°E	60	15 min linear interpolated
Dourbes	DB049	50.10°N; 4.60°E	60	15 min linear interpolated
Sodankyla	SO166	67.40°N; 26.60°E	60	15 min linear interpolated
Observatorio del Ebro	EB040	48. 40°N; 0.50°E		No ionosonde data, only TEC

[a] If data gap is larger than 1 h no interpolation has been performed (no data available).

the instrumental satellite-receiver biases are estimated simultaneously by a Kalman filter run over 24 h excluding measurements at elevation angles less than 20°. The calibrated slant TEC data are then mapped to the vertical by applying a mapping function based on a single-layer ionosphere approximation at $h = 400$ km. In a final step, the observed TEC data are merged into a regional TEC model, Neustrelitz TEC Model (NTCM2, Jakowski et al., 1998). The advantage of such an assimilation technique is that even in case of a low number of measurements reasonable ionospheric corrections can be provided to users to help them enhancing accuracy and integrity of positioning (Jakowski, 1996). The TEC data are presented in a regular grid with 2.5° and 5° grid spacing in latitude and longitude, respectively (cf. http://www.kn.nz.dlr.de/daily/tec-eu/). Since the IGS network provides about 60–200 TEC data points over the European region considered here, the technique is restricted for monitoring large-scale horizontal ionisation structures with an accuracy of $1–2 \times 10^{16}$ electrons per square metre (Jakowski and Sardón, 1996). For comparison with the ionosonde data, the corresponding TEC values are interpolated from the grid values in the vicinity of the selected ionosonde station.

At the University of Warmia and Mazury, TEC is derived from GPS measurements at ground stations of the EUREF permanent GPS network (EPN). A single-station algorithm was used for TEC calculations (Baran et al., 1997; Krankowski et al., 2007). To determine the ionospheric TEC, a geometry-free linear combination of GPS observables was used. To represent TEC over Europe, detailed TEC maps were created with observations from more than 100 GPS permanent stations. To obtain the spatial distribution of TEC we used the regional TEC model with a spherical harmonic expansion (in the geographic latitude and longitude) to degree 16 and order 16. Only GPS observations with elevation angles above 20° were used in the calculations. The dense network of GPS stations in Europe provides high spatial resolution of TEC measurements. EPN network provides spatial resolution and TEC accuracy of about 150–200 km and 1–2 TECU (1 TECU $= 1 \times 10^{16}$ electrons), respectively.

The location of the GPS-derived TEC measurements and the analysed period (October 2003) used in this paper are the same as ionosonde measurements. (Table 1). The time resolution of TEC measurements is generally $\Delta t_{\mathrm{TEC}} = 5$ min.

3. Observations

The observations are presented as spatial gradients and rate of change of peak electron density and the vertical TEC derived from vertical sounding and TEC reconstructions in October 2003. Since the number of spatial gradients is restricted to the number of station links, the resolution in azimuth is a priori rather poor. Nevertheless, the station distribution allowed the computation of well-conditioned zonal and meridional gradients of the critical frequency foF2 (or NmF2) and TEC. Spatial gradients of critical frequency between vertical sounding stations marked by j and i indexes are computed by

$$\frac{\Delta \mathrm{foF2}_{ij}}{\Delta x_{ij}} = \frac{\mathrm{foF2}_j - \mathrm{foF2}_i}{\Delta x_{ij}} \tag{1}$$

The horizontal distance Δx_{ij} is defined by the spherical distance in the ionosphere at 400 km height. The rate of change of the critical frequency at time t_k computed for a selected station is defined by

$$\frac{\Delta \mathrm{foF2}_k}{\Delta t} = \frac{\mathrm{foF2}_{k+1} - \mathrm{foF2}_{k-1}}{2\Delta t} \tag{2}$$

Following the ionosonde data time resolution, the time increment Δt, was fixed at $\Delta t_{\mathrm{VS}} = 15$ min. For reasons of comparability the corresponding TEC gradients are computed in exactly the same way. In case of separate TEC computations the higher time resolution of $\Delta t_{\mathrm{TEC}} = 5$ min is applied. It is evident that zonal gradients emphasise the diurnal variation of the ionospheric plasma density whereas meridional gradients are expected to be negative in average due to the decreasing solar zenith angle towards higher latitudes. This is confirmed by the spatial gradients of the foF2 shown in Fig. 2. Whereas the zonal link RL052–JR055 (cf. Table 1) provides strong diurnal variations symmetrically around zero, the meridional link

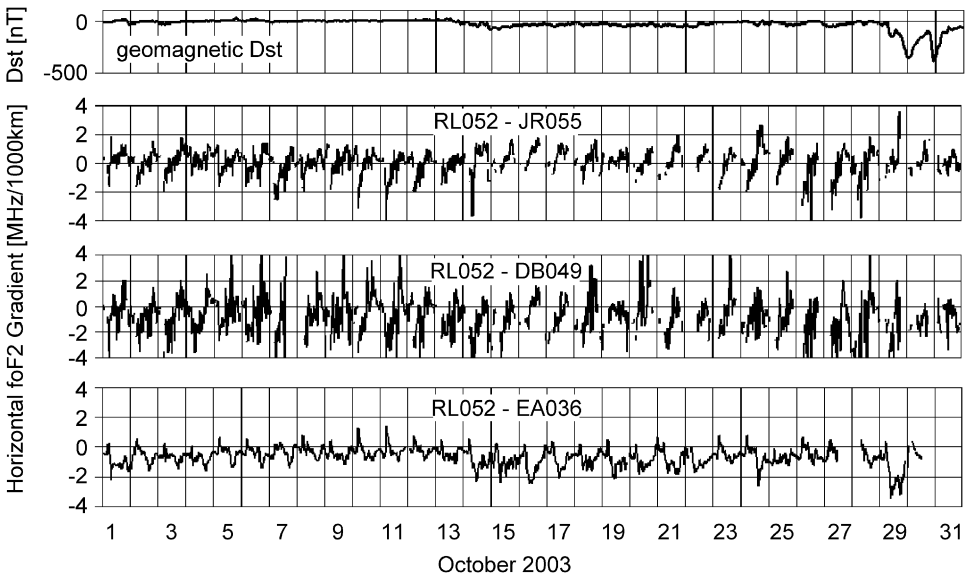

Fig. 2. Horizontal foF2 gradients in MHz/1000 km for three selected directions with the following azimuths between them RL052–JR055: 67°; RL052–DB049: 108°; and RL052–EA036: 196°. Zonal gradients are dominated by a strong diurnal effect.

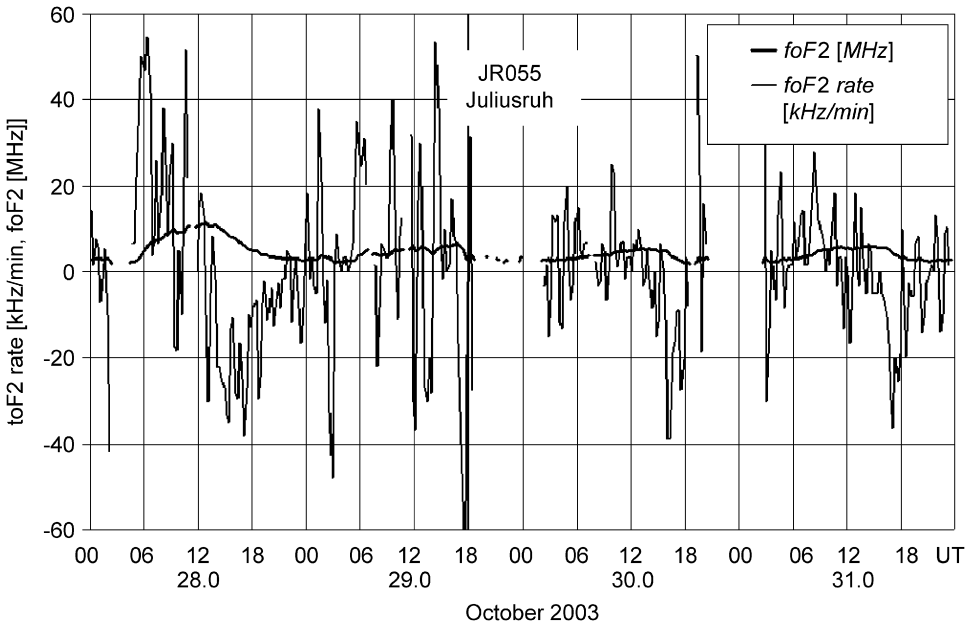

Fig. 3. foF2 rate for Juliusruh on 28–31 October 2003. While the variations are strongly irregular, enhanced amplitudes on 29 October are probably caused by autoscaling errors in foF2 data.

RL052-EA036 shows mainly negative values with reduced diurnal variation under quiet geomagnetic conditions. The geomagnetic Dst index, plotted in the uppermost panel, indicates quiet geomagnetic activity before 28 October. On 29 October a strong geomagnetic storm causes also enhanced variations in foF2 and TEC gradients. Sometimes, due to technical reasons, ionosonde data are not recorded during the storm period. It is remarkable that the typical diurnal variation disappears during the 3 storm days end of October 2003 called the Halloween storm.

The rate of change of the critical frequency derived from foF2 measurements in Juliusruh during the storm period on 28–31 October 2003 is plotted in Fig. 3. The plot demonstrates large noise in the foF2 rate of change superposed by the diurnal variation as the comparison with the original foF2 data clearly shows. Considering difficulties in ionogram data analysis during ionospheric

storms, enhanced amplitudes of the irregular rate of change on 29 October are probably due to autoscaling errors. Detection or separation of individual perturbations is difficult in ionogram analysis.

The derived gradients in foF2 can be compared with corresponding TEC values. Fig. 4 shows the horizontal gradients in TEC for the same or similar station links as shown in Fig. 2. As expected, the meridional link RL052–EB040 shows mostly negative values due to enhanced ionisation at the southern station in particular at daytime. Strong gradient amplitudes can be seen on perturbed days 29–31 October 2003. Worth notice is the observation of enhanced zonal gradient amplitudes in foF2 and TEC during the days 25–27 October 2003, a few days before the storm starts, although the D_{st} index does not show any significant perturbation (Figs. 2 and 4).

When using TEC data for further analysis, the question arises how accurate the TEC data sets originating from different sources are. To answer this question, Fig. 5 shows the original TEC data derived at DLR and UWM for the location of the ionosonde station Rome. As it can be seen, the data agree rather well with a RMS deviation of 2.3 TECU. The most pronounced deviations between both reconstructions appear during the storm on 29 October. This needs further investigation. Nevertheless, we believe that in this phase of preliminary studies on ionospheric perturbation indices the agreement is sufficient for our estimations.

As indicated in Figs. 2 and 4, ionospheric gradients are strongly developed, especially during the perturbed days at the end of October 2003. A detailed view of horizontal TEC gradients between four ionosonde station locations on 29 October is given in Fig. 6. It is interesting to note that all station links considered here show a wavelike perturbation in the TEC gradient with a periodicity of about 4 h. Since this feature is shown at all station links, the driving perturbation process is a large scale one. The highest gradients are observed in North–South direction (RL052–EB040 and JR055–RO041). The wavelike structures are well correlated and nearly in phase. The zonal gradients (RL052–JR055 and EB040–RO041) are smaller and the phase relations are more complex.

An alternative is to use squared values of the ionospheric gradients. This procedure implies two advantages:

- It removes signs naturally depending on computing the difference between stations 1 and 2 or stations 2 and 1
- It enhances the dynamic range of observed values, thus suppressing the diurnal variation and pronouncing ionospheric perturbations.

An example is given in Fig. 7 where squared horizontal TEC gradients between the same ionosonde stations as

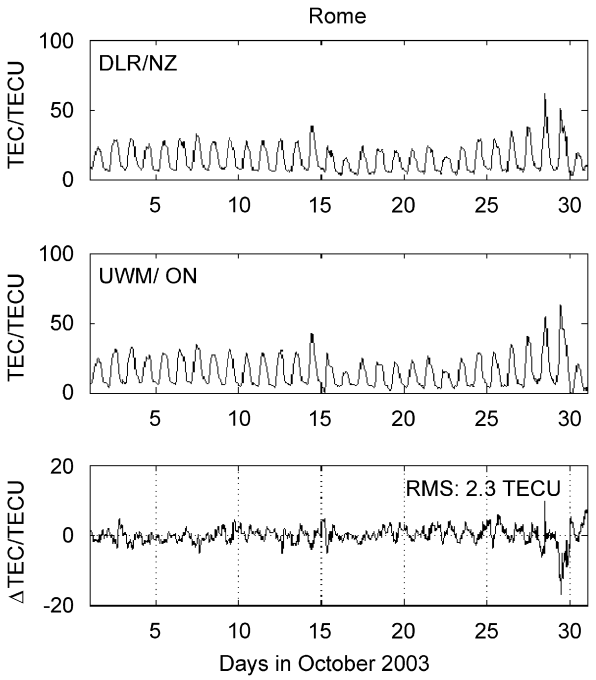

Fig. 5. Comparison of original TEC values derived for the Rome ionosonde station location in DLR/Neustrelitz and UWM/Olzstyn. The lower panel shows the deviation ΔTEC = TEC(DLR)−TEC(UWM), the standard deviation is 2.3 TECU.

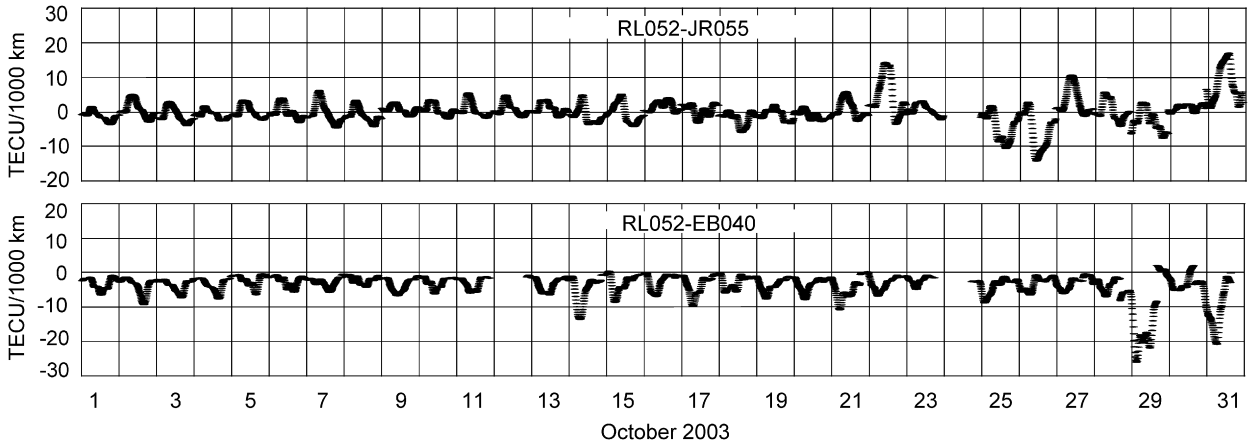

Fig. 4. TEC gradients corresponding to Fig. 2 (UWM).

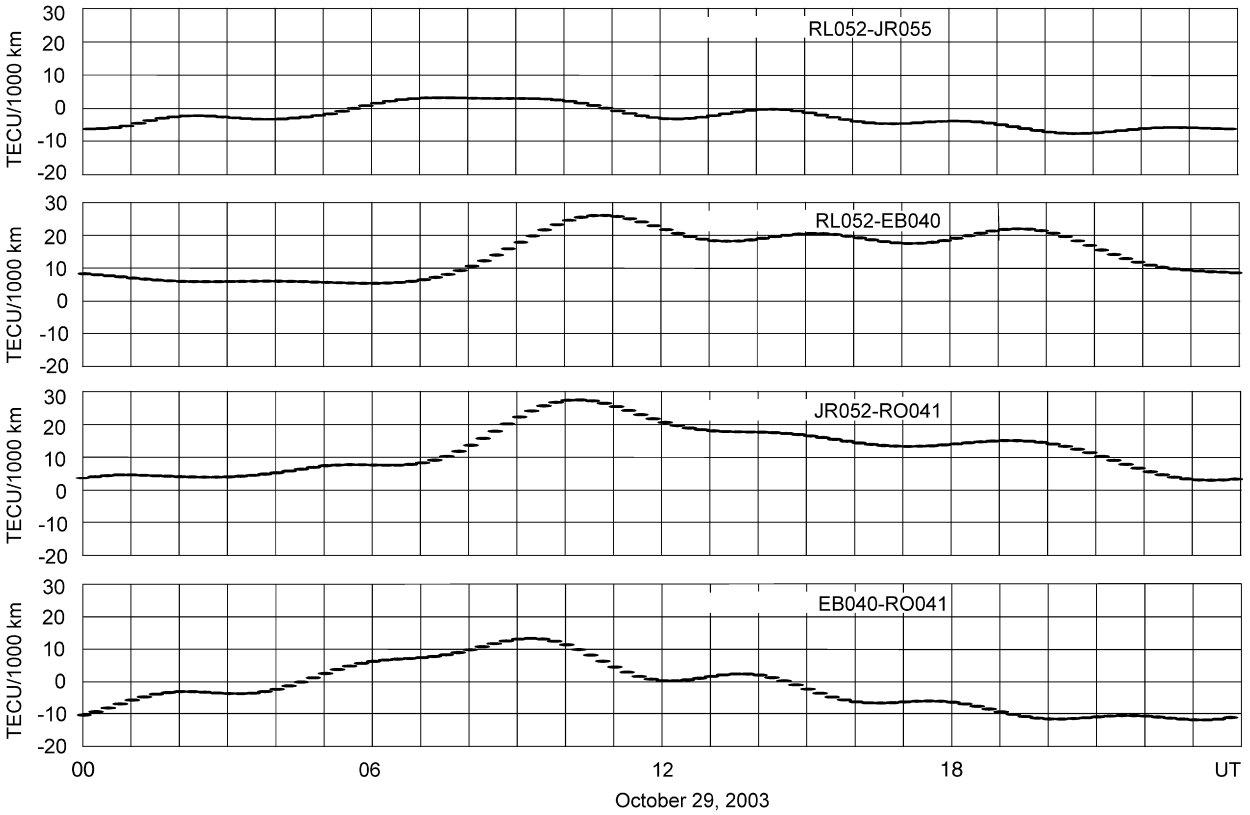

Fig. 6. Wavelike phenomena in GPS-derived TEC gradients at four station links on 29 October 2003 (UWM).

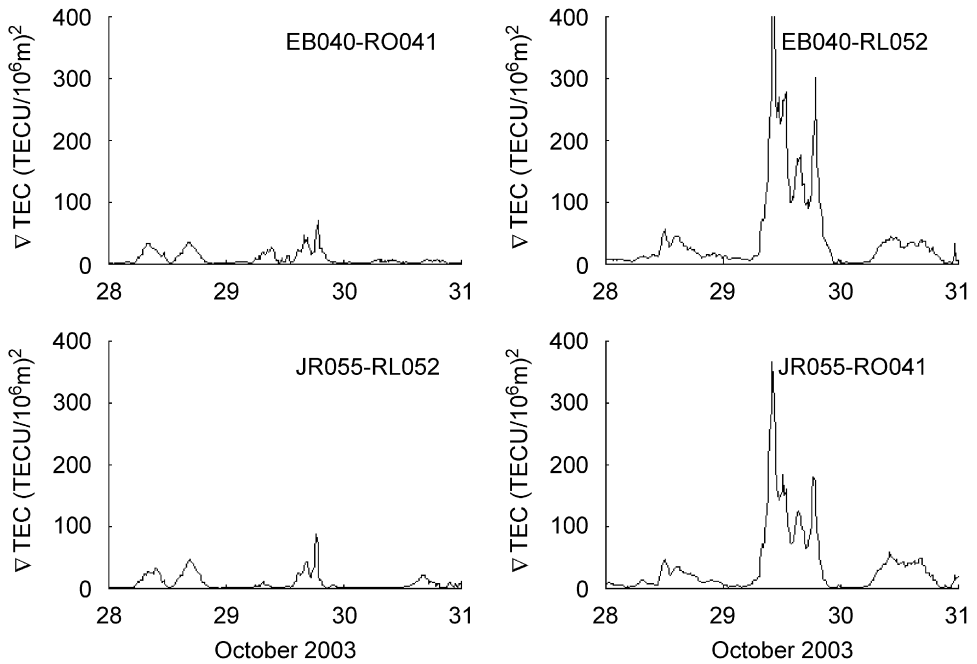

Fig. 7. Squared TEC gradients on 29 October 2003 at four station links (DLR).

selected in the previous Fig. 6 are shown. It is interesting to see that the squared TEC gradients representing zonal gradients on the left side are much smaller on 29 October than the corresponding values for latitudinal gradients shown at the right side. This clearly indicates that the major ionospheric perturbation is developing in

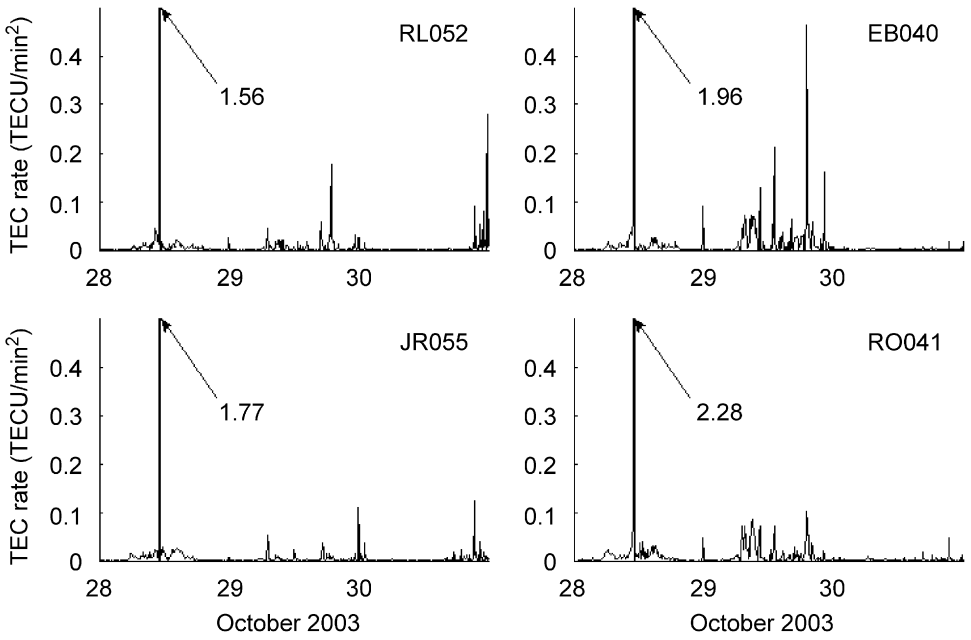

Fig. 8. Squared TEC rate derived at four stations for 28–30 October 2003 (DLR).

North–South direction. The wavelike phenomena occurring on 29 October 2003 as shown in Fig. 6, are better visible in this presentation. Remarkable is the strong coherence of TEC variation at meridional links separated by about 15° in longitude or 1 h local time difference. Quadratic terms may also be computed for the rate of change. The squared rate of change of TEC derived at the geographic locations of ionosonde stations RL052, JR040, EB040 and RO041 for the perturbation period 28–30 October 2003 is shown in Fig. 8. As in case of the squared gradients, the squared rates do not distinguish between signs, i.e. the parameter pronounces only rapid changes ignoring increasing and decreasing behaviour of TEC. An extremely large signal up to about 4 $(\mathrm{TECU/min})^2$ is shown during the large solar flare at 11:05 UT on 28 October 2003. The storm-related maximum amplitudes observed here are about 1/10 of the flare-induced rate.

Comparing the values at different stations it is apparent that the squared TEC rate is stronger at the lower latitude stations, probably due to the higher ionisation. The storm pattern derived for different stations are of low coherence. It is worth noting that the perturbation pattern just before midnight on 30 October 2003 is only visible at the northern stations RL052 and JR055. This indicates a perturbation, which is restricted to high latitudes, at least within the observation period.

4. Results and discussion

The vertical incidence sounding and TEC observations and their spatial and temporal derivatives monitored over 31 days of October 2003 provide comprehensive information on the ionospheric state. Whereas the ionosonde data provide local plasma density information, the TEC data give integral information on the mainly spherically structured ionosphere. When combining these parameters, a new parameter, the equivalent slab thickness may be derived that provides additional information about the width of the vertical electron density profile (e.g. Miro et al., 1999). The equivalent slab thickness reacts sensitive to dynamic forces such as neutral winds and electric fields. These forces may even lead to opposite temporal variation of TEC and foF2 (Jakowski and Lois, 1984) either by strong compression of the ionosphere (increase of foF2 and reduction of TEC) or expansion of the ionosphere (decrease of foF2 and increase of TEC). Considering the slab thickness avoids misinterpretation and helps to explain the physical background of ionospheric storms.

Due to the sparseness of the ionosonde network the investigation is restricted on large-scale aspects of horizontal plasma density gradients. Both the vertical sounding as well as the TEC data indicates enhanced spatial gradients and rate of change in the course of the severe geomagnetic storm end of October 2003. This is a well-known effect closely related to severe 4D ionospheric electron density perturbations during geomagnetic storms (e.g. Cander and Mihajlovic, 1998; Foerster and Jakowski, 2000; Nava et al., 2007).

Ionospheric perturbations may appear even under quiet geomagnetic conditions a few days before the large storm, as indicated here. The short-term decorrelation of ionospheric and geomagnetic perturbations is evident during the solar flare effect on 28 October 2003 at 11:05 UT (cf. Fig. 8). This underlines the necessity of a specific ionospheric perturbation index (Jakowski et al., 2005; Bremer et al., 2006) for improving accuracy and

safety of operational radio systems that are sensitive to ionospheric impact.

Spatial and gradients and rate of change of key plasma parameters such as the electron density NmF2 or its vertical integral, TEC, are promising for defining such an index. As Fig. 9 shows, the quadratic mean of the foF2 rate clearly enhances during the ionospheric storm at all ionosonde stations considered in this study. Unfortunately, the foF2 rate of change is difficult to determine during ionospheric perturbations (cf. Fig. 3). This may generate some problems in operational observations.

Squared spatial gradients and rate of change of TEC have demonstrated (Figs. 7 and 8) to be promising candidates for defining a perturbation index. Quadratic terms enhance large perturbation-induced values and suppress small amplitudes e.g. caused by diurnal variation. The sharp structures visible in the squared TEC gradients are very helpful for recognising ionospheric perturbations.

It is worth notice that this study also shows that different technologies used for deriving TEC from ground-based GNSS measurements in DLR and UWM lead to comparable results. Further improvements in comparability of TEC retrievals are expected in the next years. TEC measurements have the advantage that they are more robust than vertical sounding measurements.

Coming back to the spatial gradients and rate of change of TEC as shown in Figs. 6–8, the observations show that the Halloween storm is mainly structured in the North–South direction (Fig. 10). This has been expected and is in agreement with numerous storm-related studies. To study this structure in more detail, we have plotted the analysed spatial gradients from foF2 and TEC

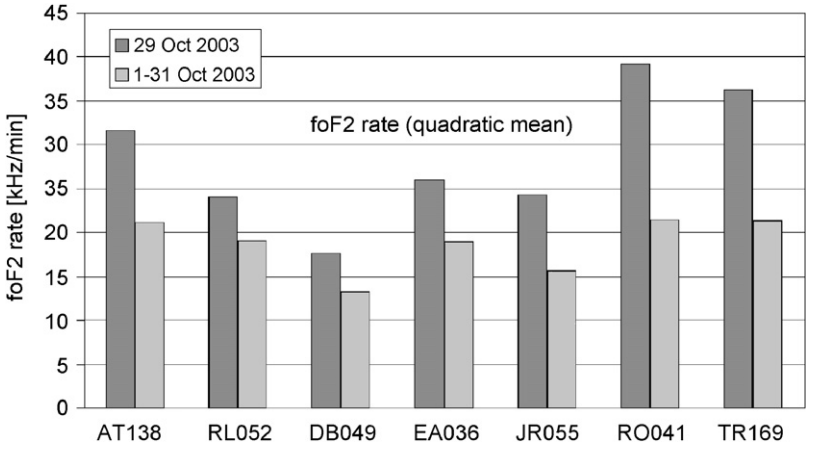

Fig. 9. foF2 shown as quadratic mean is increased in the order of 25–90% at all ionosonde stations during 29 October compared with the monthly average. The monthly average value amounts to about 18 kHz/min.

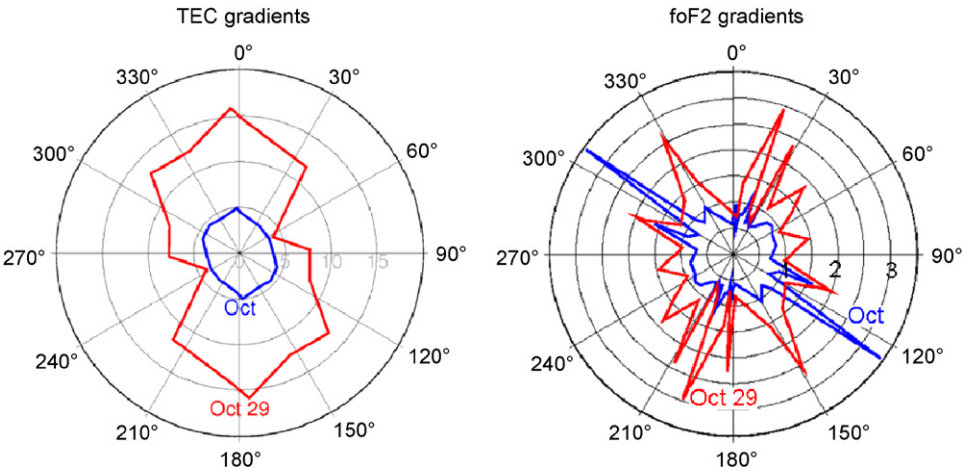

Fig. 10. Azimuthal distribution of horizontal ionisation gradients of TEC (UWM) and foF2 over Europe. Presented is the quadratic mean of TEC (TECU/1000 km) and foF2 (MHz/1000 km) on 29 October and for the entire month. The extreme foF2 gradient in Northwest–Southeast direction is related to high latitude stations TR169 and SO166 whose distance is less than 500 km.

measurements deduced for storm days 29–31 October 2003 as a function of the azimuth of link direction. In agreement with observations presented in Section 3, the spatial gradients are largest on 29 October 2003 during the positive storm phase (cf. Foerster and Jakowski, 2000; Jakowski et al., 1999). Subsequently, the amplitude of gradients decreases systematically due to the enhanced plasma loss caused by the storm-induced enrichment of molecular constituents in the lower ionosphere (e.g. Prölss et al., 1991). As discussed earlier, the latitudinal gradients are significantly stronger than the zonal gradients, for TEC approximately by a factor of 2. The ionosonde data indicate also an increase of the gradient in North–South direction compared with East–West gradients but the data situation is rather poor to more quantify this.

Besides this fact it becomes evident that the gradient distribution on 29 October as well as the monthly averages indicate a slight asymmetry with respect to the geographic North–South direction. Because the azimuthal resolution of data is rather poor, this deviation is probably within the uncertainty of measurements. To find out whether this asymmetry might be related to the declination of the geomagnetic field, more detailed studies would be needed in a mid-latitude region with more pronounced declination of the geomagnetic field.

5. Conclusions

Spatial gradients and rate of change of foF2 and TEC have been investigated using data from European ionosonde station sites during October 2003. Ionospheric storms and irregularities are characterised by enhanced ionisation and redistribution of plasma due to perturbation-induced forces such as electric fields and thermospheric winds. Their scale size ranges from meter level up to several thousands of kilometres. The coverage of ionosonde stations used in this study enabled studying only large-scale storm behaviour in terms of spatial gradients and rate of change. Gradients are able to characterise structure and dynamics of ionospheric storms effectively. Furthermore, spatial and temporal derivatives of plasma parameters such as NmF2 and TEC are of particular interest in applications such as space-based navigation and positioning. Hence, horizontal gradients and rate of change of ionisation are good candidates for defining perturbation indices to characterise the perturbation degree of the ionosphere with only a few data. The results of this study show that the spatial gradients and rate of change of foF2 characterise ionospheric storms by enhanced values, which may be difficult to determine from perturbed ionograms.

Two different approaches for determining TEC have revealed similar results. Although further improvements still need to be done, it can be concluded that TEC-based methods can be used as a platform for introducing ionospheric perturbation indices on international level. The combination of TEC with vertical sounding data enables the estimation of the equivalent slab thickness, which is a key parameter in studying ionospheric perturbation processes. It is recommended to study these relationships in more detail in future work.

It has been demonstrated that squared TEC-rate and -gradient values may provide excellent perturbation information for GNSS users. The study favours latitudinal TEC gradient as being a good candidate for defining a perturbation index at least for the European area.

Perturbation-induced spatial gradients of TEC and foF2 maximise in North–South direction, exceeding average and East–West gradients approximately by a factor of 2 for TEC.

Acknowledgements

The authors are grateful to the COST 296 action for supporting the cooperative work. We thank IGS and EUREF networks and data centres for making available numerous GPS and ionosonde data.

References

Baran, L.W., Shagimuratov, I.I., Tepenitzina, N.J., 1997. The use of GPS for ionospheric studies. Artificial Satellites 32 (1), 49–60.

Bremer, J., Cander, Lj.R., Mielich, J., Stamper, R., 2006. Derivation and test of ionospheric activity indices from real-time ionosonde observations in the European region. Journal of Atmospheric and Solar-Terrestrial Physics.

Cander, Lj.R., 1993. On the global and regional behavior of the mid-latitude ionosphere. Journal of Atmospheric and Terrestrial Physics 55 (11–12), 1543–1551.

Cander, Lj.R., Mihajlovic, S.J., 1998. Forecasting ionospheric structure during the great geomagnetic storms. Journal of Geophysical Research 103 (A1), 391–398.

Conkright, R.O., McNamara, L.F., 1997. Quality control of automatically scaled vertical incidence ionogram data. Radio Science 32 (5), 1997–2002.

Foerster, M., Jakowski, N., 2000. Geomagnetic storm effects on the topside ionosphere and plasmasphere: a compact tutorial and new results. Surveys in Geophysics 21 (1), 47–87.

Jakowski, N., 1996. TEC monitoring by using satellite positioning systems, modern ionospheric science. In: Kohl, H., Rüster, R., Schlegel, K. (Eds.), EGS, Katlenburg-Lindau. ProduServ GmbH Verlagsservice, Berlin, pp. 371–390.

Jakowski, N., Lois, L., 1984. Investigation of Ionospheric Storms by Combining Ionospheric Total Electron Content with foF2-Data, observed in Havana/Cuba between July 1974 and December 1977. Gerlands Beitrage Zur Geophysik 93, 1–11.

Jakowski, N., Sardón, E., 1996. Comparison of GPS/IGS-Derived TEC Data with Parameters Measured by Independent Ionospheric Probing Techniques. In: Proceedings of IGS, 19–21 March, 1996, Silver Springs, pp. 221–230.

Jakowski, N., Sardon, E., Schlueter, S., 1998. GPS-based TEC observations in comparison with IRI95 and the European TEC Model NTCM2. Advances in Space Research 22, 803–806.

Jakowski, N., Schlueter, S., Sardon, E., 1999. Total Electron Content of the ionosphere during the geomagnetic storm on January 10, 1997. Journal of Atmospheric and Solar-Terrestrial Physics 61, 299–307.

Jakowski, N., Stankov, S.M., Klaehn, D., 2005. Operational space weather service for GNSS precise positioning. Annales Geophysicae 23, 3071–3079.

Jakowski, N., Stankov, S.M., Schlueter, S., Klaehn, D., 2006. On developing a new ionospheric perturbation index for space weather operations. Advances in Space Research 38 (11), 2596–2600.

Krankowski, A., Shagimuratov, I.I., Baran, L.W., 2007. Mapping of foF2 over Europe based on GPS-derived TEC data. Advances in Space Research 39, 651–660.

Menvielle, M., Berthelier, A., 1991. The K-derived planetary indices: description and availability. Reviews of Geophysics 29 (3), 415–432.

Miro, G., Jakowski, N., de la Morena, B.A., 1999. Equivalent slab thickness of the ionosphere in middle latitudes based on TEC/f0F2 observations over EL Arenosillo. In: Hanbaba, R., B.A. de la Morena, B.A. (Eds.), Proceedings of Third COST251 Workshop, September, 1998, pp. 87–92.

Nava, B., Radicella, S.M., Leitinger, R., Coïsson, P., 2007. Use of Total Electron Content data to analyze ionosphere electron density gradients. Advances in Space Research 39, 1292–1297.

Prölss, G.W., Brace, L.H., Mayr, H.G., Carignan, G.R., Killeen, T.L., Klobuchar, J.A., 1991. Ionospheric Storm Effects at Subauroral Latitude: A Case Study. Journal of Geophysical Research 96, 1275–1288.

Skone, S., Kundsen, K., de Jong, M., 2001. Limitations in GPS receiver tracking performance under ionospheric scintillation conditions. Physics and Chemistry of the Earth Part A 26, 613–621.

Stankov, S.M., Jakowski, N., Tsybulya, K., Wilken, V., 2006. Monitoring the generation and propagation of ionospheric disturbances and effects on GNSS positioning. Radio Science 41, RS6S09.

Further reading

Websites of ionosonde data centers

WDC-C1 〈http://www.ukssdc.ac.uk/wdcc1/iono_menu.html〉.
SPIDR 〈http://spidr.ngdc.noaa.gov/spidr/index.jsp〉.
Sodankyla Geophysical Observatory 〈http://www.sgo.fi/Data/Ionosonde/ionArchive.php〉.